ADVANCED FUNCTIONAL MATERIALS

DOI: 10.1002/adfm.200701459

Effects of Solvent Mixtures on the Nanoscale Phase Separation in Polymer Solar Cells**

By *Yan Yao, Jianhui Hou, Zheng Xu, Gang Li,* and *Yang Yang**

The mixed solvent approach has been demonstrated as a promising method to modify nanomorphology in polymer solar cells. This work aims to understand the unique role of the additive in the mixture solvent and how the optimized nanoscale phase separation develops laterally and vertically during the non-equilibrium spin-coating process. We found the donor/acceptor components in the active layer can phase separate into an optimum morphology with the additive. Supported by AFM, TEM and XPS results, we proposed a model and identified relevant parameters for the additive such as solubility and vapor pressures. Other additives are discovered to show the ability to improve polymer solar cell performance as well.

1. Introduction

A remarkable improvement in the device performance of polymer solar cells has been achieved since photo-induced electron transfer from conjugated polymer to fullerene was first reported in 1992.[1] After over a decade of development, there have been reports on polymer solar cells with power conversion efficiencies of around 6%.[2] The progress in this field has been achieved through enormous efforts in the design of new low band-gap polymer materials,[3–8] improvement in the understanding of bulk-heterojunction device physics,[9] morphology,[10–13] novel device fabrication methods[14,15] and structures.[16–18]

The bulk-heterojunction approach has remained the prime candidate for high efficiency polymer solar cells since its introduction in 1995.[19,20] By intermixing a conjugated polymer with C_{60} molecules or their methanofullerene derivatives, efficient exciton dissociation is achieved at the large interfacial area, overcoming the limited exciton diffusion length in the polymer. On the other hand, continuous pathways for the transportation of both electrons and holes are crucial and must be both controlled and enhanced in order to allow thick films to maximize absorption without significant recombination loss.[9] It is agreed that the optimum nanoscale morphology must be a balance between a large interfacial area and continuous pathways for carrier transportation.[21] In the most extensively studied polymer solar cell model system, regioregular poly(3-hexylthiophene) (P3HT): [6,6]-phenyl C_{61} butyric acid methyl ester (PCBM) system, initial photovoltaic devices fabricated without any post-treatment show low efficiency due to unoptimized morphology.[22] PCBM is finely dispersed between P3HT chains, thus suppressing P3HT crystallite formation.[22] To ''heal'' the disordered polymer chain, PCBM must be redistributed (demixing) to allow better polymer chain alignment. Two approaches have been reported effective in reshaping PCBM distribution: ''thermal annealing'' and ''solvent annealing''. In 2003, Padinger et al. reported 3.5% power conversion efficiency (PCE) by annealing a P3HT:PCBM blend.[14] This demonstration led to extensive studies on the ''thermal annealing'' approach, and PCE values up to 5% were reported.[23] The ''solvent annealing'' approach was recently proposed by Li et al.[15] Self-organization in polymer chains was achieved by controlling polymer layer growth rate from the solution to the solid state.[12]

In addition to the above methods, mixture solvent approach represents one new promising method to modify solar cell morphology and improve device performance. Zhang et al. found a significant enhancement in photocurrent density in polyfluorene compolymer/fullerene blends when introducing a small amount of chlorobenzene into chloroform solvent.[24] Time-resolved spectroscopy on the picosecond time scale shows that charge mobility was influenced by the mixing solvents. Recently, Peet et al. reported that adding alkanethiol to P3HT/PCBM in toluene can enhance device performance due to longer carrier lifetime with ordered structure in morphology.[25] Alkanethiol is also found effective to achieve the highest efficiency record for low band gap polymer solar cells.[26] However, there are several questions remaining

[*] Prof. Y. Yang, Dr. Y. Yao, Dr. J. Hou, Z. Xu
Department of Materials Science and Engineering and
California Nanosystems Institute
University of California Los Angeles
Los Angeles, CA 90095 (USA)
E-mail: yangy@ucla.edu
Dr. G. Li
Solarmer Energy Inc.
El Monte, CA 91731 (USA)

[**] This work was financially supported by Solarmer Energy Inc., UC Discovery Grant (Grant No. GCP05-10208), and Office of Navy Research (Grant No. N00014-01-1-0136, program manager Dr. Paul Armistead). We appreciate Mr. Hyun Cheol Lee for the help on TEM measurement and Dr. Yue Wu for helpful discussion.

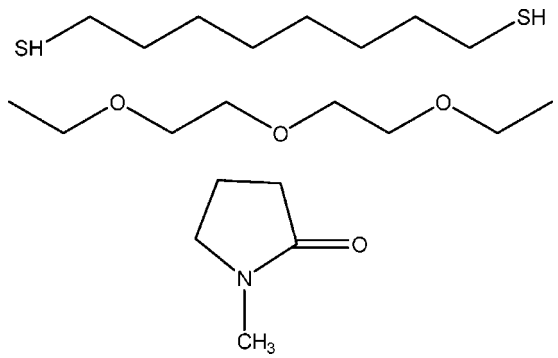

Figure 1. Chemical structures of 1,8-octanedithiol, di(ethylene glycol)-diethyl ether, and N-methyl-2-pyrrolidinone.

unanswered: (i) How does the optimized morphology develop during spin-coating process when alkanethiol exists? (ii) What is the function of alkanethiol in the mixture solvent and which properties of alkanethiol are relevant for the improvement? (iii) Can we find some alternative mixture solvents to achieve similar function as alkanethiol?

Spin-coating process for the polymer/fullerene blend system in the mixture solvent is a complex process because it is a non-equilibrium state that both thermodynamic and kinetic parameters can influence phase separation, and the system contains four components with dissimilar physical/chemical properties. The present work aims to understand the unique role of the additive behind the improvement and provide some tentative answers to the above questions. In the work reported in the following manuscript, we first conducted an in-depth investigation of the function of 1,8-octanedithiol (OT, with its chemical structure shown in Fig. 1) in the model system (P3HT:PCBM) using atomic force microscopy (AFM) and transmission electron microscopy (TEM), X-ray photoelectron spectroscopy (XPS) combined with optical absorption and electrical measurement. We demonstrated that P3HT:PCBM with OT can phase separate into an optimized morphology during spin-coating process. Then we identified relevant properties of OT and proposed the mechanism of how the optimized morphology was achieved. Finally, we report two additives (shown in Fig. 1) that have similar abilities as OT to increase device performance. The model proposed here will enable us gain insights of the mixture solvent approach in finely controlling nanomorphology in polymer solar cells.

2. Results and Discussion

Figure 2a shows the UV-Visible absorption spectroscopy of P3HT:PCBM films of various PCBM loading ratio (33, 50, 67 wt %) processed with OT as an additive. The concentration of OT is 9.7 mg ml^{-1} in all different PCBM loadings. The films were obtained by spin-coating the blend solution at 2000 rpm for 60 s. At this spin-coating setting, all the films solidified immediately after spin-coating and no further color change was observed.[12] P3HT film shows three features in absorption: two peaks at 510 and 550 nm and one shoulder at 610 nm due to strong inter-chain interactions.[27] When the loading of PCBM is increased, its absorption peak at 330 nm becomes more pronounced. However, it is surprising that the shape of P3HT peaks remains unchanged at higher PCBM loading. The addition of OT therefore provides the similar function of preserving P3HT crystallinity in P3HT:PCBM blend as achieved in the "solvent annealing" approach[12] For comparison, the films processed without OT addition are shown in Figure 2b. It is quite clear that P3HT absorption peaks blue-shift at heavier PCBM loading and the originally strong vibronic shoulders diminish significantly. The effect of OT on the absorption of pure P3HT (solid lines in both Fig. 1a and b) is rather small because the high regioregularity P3HT has an intrinsic property to self-organize into microcrystalline domains[28] even without any additive. However, the difference at higher PCBM loadings (Fig. 1a and b) becomes more pronounced. The loss of ordering was ascribed to the fact that PCBM is finely dispersed on a molecular basis between P3HT

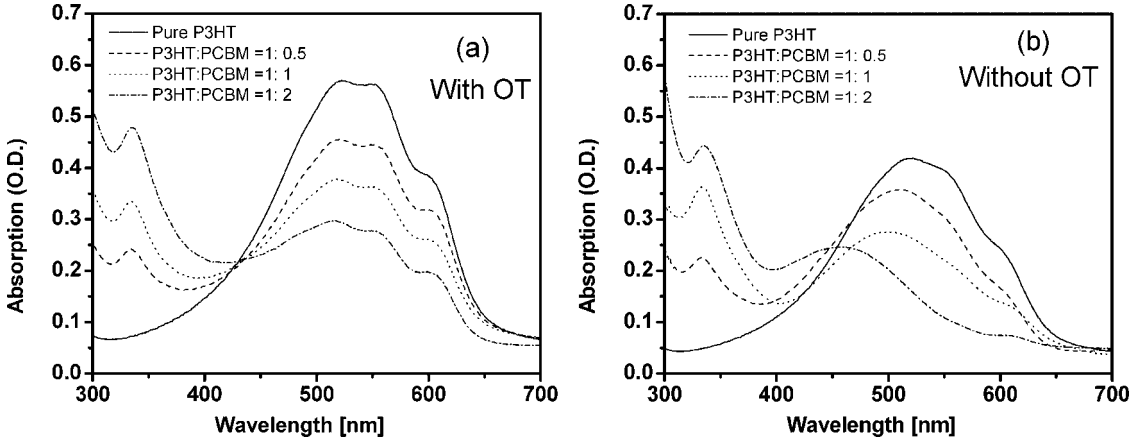

Figure 2. Absorption of P3HT:PCBM composite layer of pure P3HT (solid line), P3HT:PCBM weight ratio 1:0.5 (dashed line), 1:1 (dotted line), and 1:2 (dashed-dotted line) processed with (a) and without (b) 1,8-octanedithiol in the blend solution.

ADVANCED FUNCTIONAL MATERIALS

chains, thus preventing P3HT crystallizing.[22] It is therefore conjectured that the remarkable ability of OT is related to its capability to redistribute PCBM and P3HT in the composite film.

To test the hypothesis, we characterize the morphology of the P3HT:PCBM composite film using AFM. The film preparation conditions for AFM images were kept the same as those in device fabrication for accurate comparison. Figure 3 shows the typical height and phase images of blend films processed with and without OT (image size 1 μm × 1 μm). Two features are observed from the comparison: (i) From the height images, the surface processed with OT is significantly rougher than that without OT, with root-mean-squared surface roughness of 4.0 nm (Fig. 3a) compared to 0.7 nm (Fig. 3b). Islands and valleys are apparent in Figure 3a. It has been reported that a rough surface is a ''signature'' of high efficiency solar cells both in ''thermal annealing''[29] and ''solvent annealing''.[15] (ii) From the phase images, highly ordered fibrillar crystalline domains of P3HT are clearly visible in Figure 3c, but they are absent in Figure 3d. This suggests that highly ordered P3HT chain alignment is achieved when OT is added in the mixture, which is also consistent with the optical absorption measurements.

While AFM is employed to probe the surface of active layer, TEM provides vertical direction information by acquisition of electrons projected through the entire film.[30] TEM has been used to distinguish P3HT from PCBM due to their different densities: PCBM is 1.5 g cm^{-3} and P3HT is 1.1 g cm^{-3}.[31] We prepared our specimens for TEM measurements by spin-casting the blend solution at 2000 rpm on glass substrate, followed by floating the film on a water surface, and transferring to TEM grids. Typical bright-field TEM images for samples processed with OT are shown in Figure 4a and c. The most pronounced feature compared to samples without OT (Fig. 4b and d) is the appearance of dark clusters in the film and high contrast of these clusters to the background. These clusters are reminiscent of TEM images by Yang et al.,[31] in which PCBM-rich domains were developed during the annealing step. Similar to Yang's work, the dark regions in Figure 4a are attributed as PCBM clusters. For comparison, pure P3HT film (Fig. 4e) is very homogeneous and of low contrast, while pure PCBM (Fig. 4f) forms small crystallites

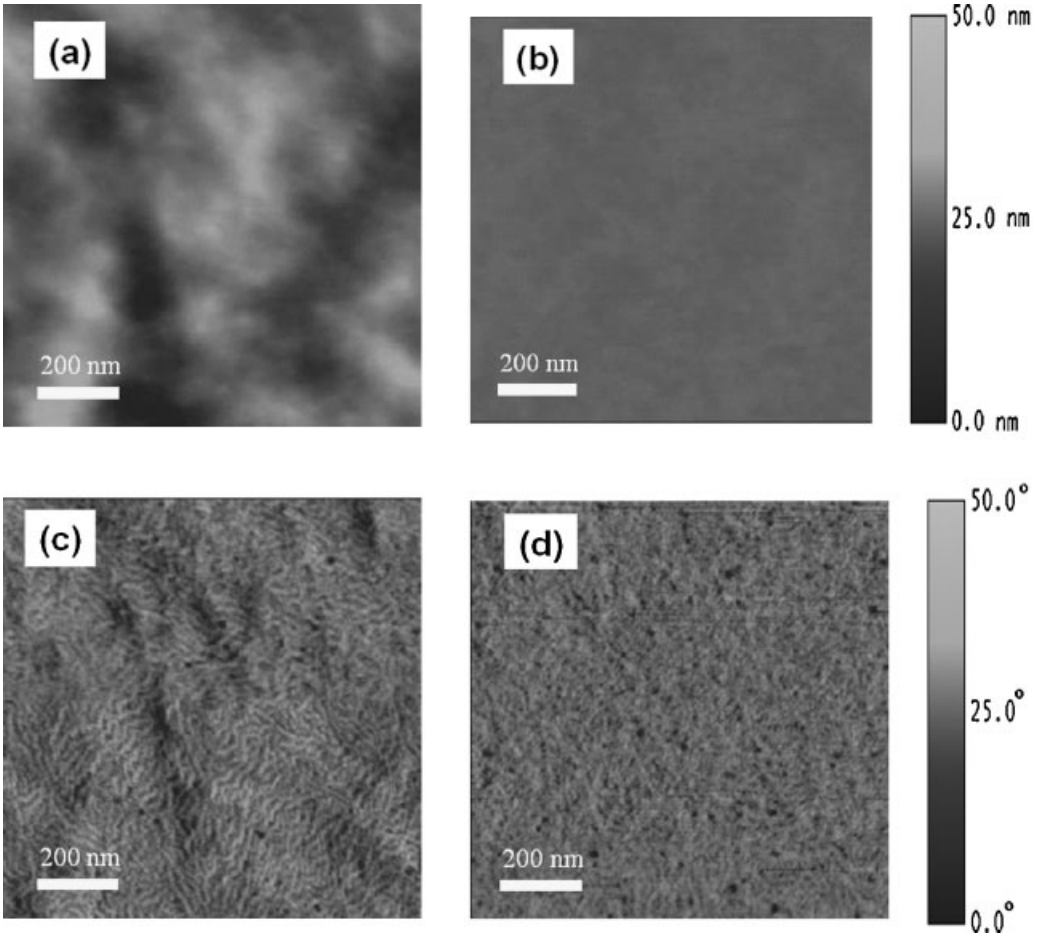

Figure 3. AFM images of P3HT:PCBM films spin-coated from dichorobenzene with ((a) and (c)) and without ((b) and (d)) 1,8-octanedithiol. (a) and (b) are height images, and (c) and (d) are phase images. The surface processed with OT is rougher than that without OT, with root-mean-squared surface roughness 4.0 nm (a) compared to 0.7 nm (b); ordered fibrillar crystalline domains of P3HT are clearly visible in (c), but they are absent in (d).

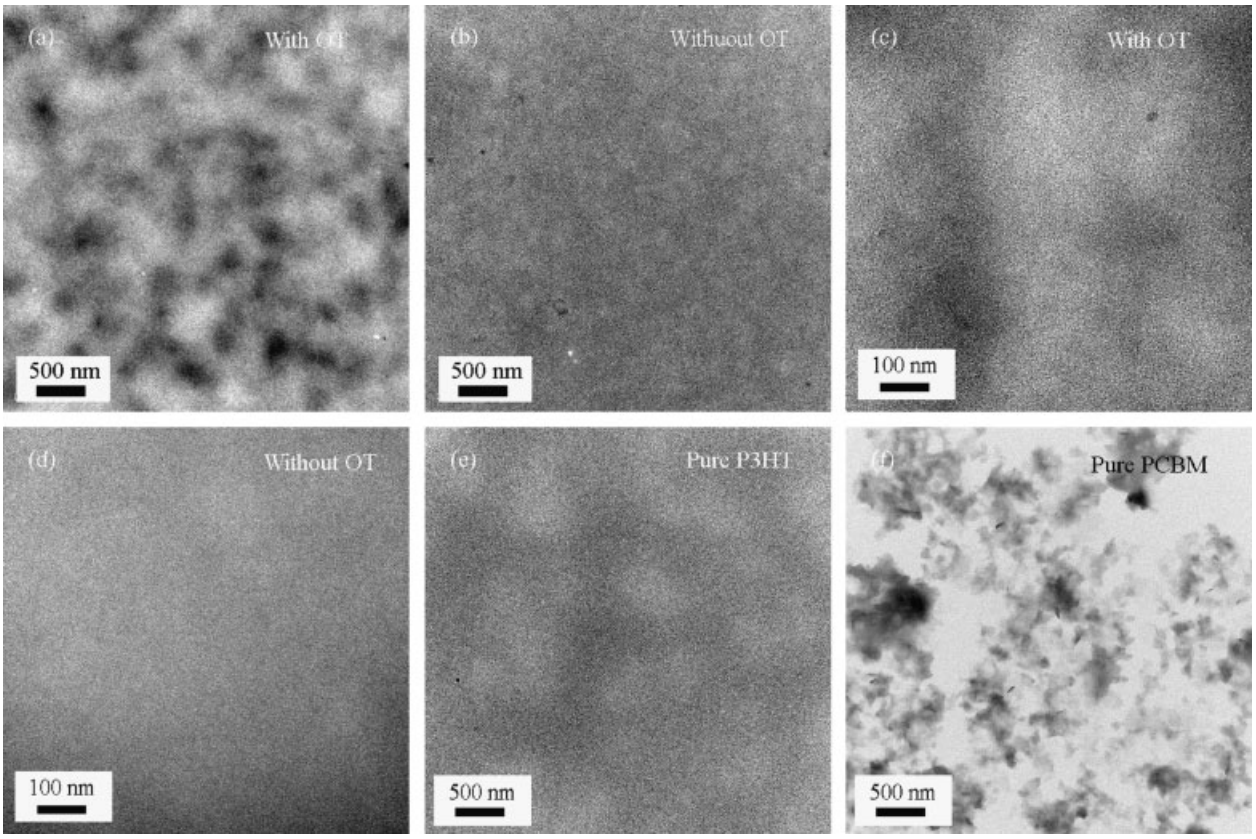

Figure 4. Bright-field TEM images of P3HT:PCBM blend film (1:1 wt. ratio) processed with (a) and without (b) 1,8-octanedithiol additive. (c) and (d) are the zoom-in images of (a) and (b). (e) and (f) correspond to pure P3HT and PCBM samples, respectively.

with high contrast. The zoomed-in image (Fig. 4c) shows pronounced fibrillar P3HT crystals, suggesting the crystallinity has been improved compared to pristine film (Fig. 4d). To rationalize the change in morphology, we infer that the solubility of PCBM in OT plays an important role in the kinetics of the spin-coating process. The solubility of PCBM in OT and DCB was measured as follows: first, the optical densities of several concentrations of PCBM solutions in toluene were measured to create a calibration curve. PCBM powder was then added into DCB and OT, respectively, to make a saturated solution and was centrifuged at 13500 rpm for 15 min. Finally, the top clear solution in the centrifuge tube was diluted to measure its absorption, and compared to the calibration curve. Results show that the solubility of PCBM in OT (19 mg ml^{-1}) is much smaller than that in DCB (100 mg ml^{-1}), which also hints at the PCBM clusters shown in TEM images.

To further characterize the active layer in the vertical direction, we conducted XPS measurement on the top and bottom surfaces of the active layer to determine the polymer/fullerene composition. The bottom surface was exposed by using the "floating off" method in water and collected on a TEM grid. Table 1 shows the results of peak area ratios of the S(2p) and C(1s) peaks for the top and bottom surfaces. The S(2p) peak originates from P3HT and is interpreted as a signature of polymer. Even though PCBM contains oxygen, O(1s) cannot unambiguously be assigned to PCBM due to the air contamination of sample. Since C(1s) peak represents the total content of P3HT and PCBM, S(2p)/C(1s) peak area ratio hence can be proportionally correlated to the P3HT concentration in the blend. From Table 1 when no OT exists in the solution, we found S(2p)/C(1s) ratio in the top and bottom surfaces is very close, indicating a homogeneous distribution of P3HT in the vertical direction. However in the mixture solvent with OT, S(2p)/C(1s) ratio for the top surface is higher than that of the bottom, suggesting P3HT enriched region in the surface and depleted region in the bottom. The observed vertical phase separation agrees well with other polymer/PCBM systems detected using dynamic TOF-SIMS[32] and UPS.[33] However, an enrichment of polymer at the bottom

Table 1. Area ratio of S(2p) peak and C(1s) peak for the top and bottom surfaces.

Peak area ratio of S(2p)/C(1s)	Top Surface	Bottom Surface
Without 1,8-octanedithiol	0.132	0.130
With 1,8-octanedithiol	0140	0.106

ADVANCED FUNCTIONAL MATERIALS

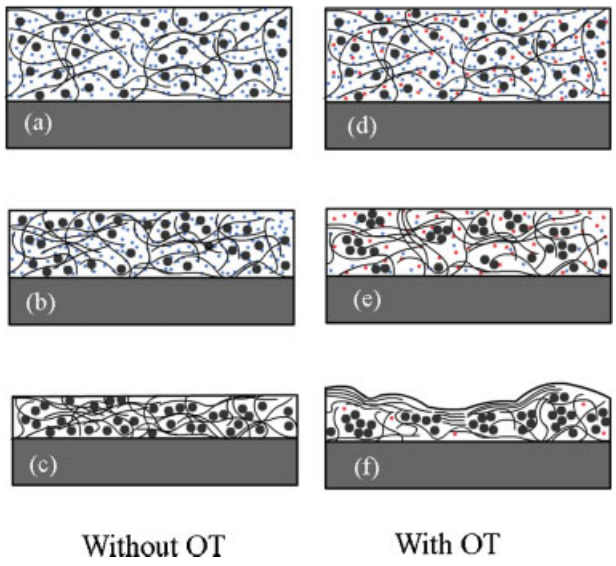

Figure 5. Proposed model during spin-coating process. Black wire: P3HT polymer chain; Big black dots: PCBM; blue dots: DCB molecules; and red dots: 1,8-octanedithiol molecules. (a–c) correspond to three stages in the spin-coating process when DCB is the sole solvent; (d–f) correspond to three stages in the spin-coating process when octanedithiol is added in DCB. Note the difference of PCBM distribution in the final stage of each case, (c) and (f). The total numbers of big black dots are same in all the images.

surface would be expected for better charge collection when PEDOT:PSS coated ITO is used as substrates. The observed vertical phase separation makes it ideal for an inverted solar cell structure[17] and we recently have achieved more than 72% external quantum efficiency in inverted device structure.[34]

Combining all the above mentioned results, we propose a model in the following and illustrate it in Figure 5 to explain the above results. When P3HT and PCBM are dissolved in the DCB (Fig. 5a, blue dots), polymer chains extend freely in the solvent and do not interact with PCBM. During spin-coating, when DCB is extracted rapidly (Fig. 5b), the whole system is quenched into a metastable state and PCBM molecules are finely dispersed between P3HT chains, interrupting the ordering of P3HT chains[21] (Fig. 5c). This is supported by the blue-shifted absorption, smooth AFM morphology and homogeneous TEM images. However, when a small amount of OT (Fig. 5d, red dots) is present in the mixture solvent, the situation is different. Because the vapor pressure of DCB is 200 times higher than OT at room temperature as shown in Table 2, DCB will evaporate much faster than OT during spin-coating,

Table 2. Boiling points, vapor pressure and PCBM solubility of DCB, OT, DEGDE and NMP. (Boiling points and vapor pressure are from Handbook of Chemistry and Physics, 82th ed.)

Solvent	Boiling points [°C]	Vapor pressure at 30 °C [Pa]	PCBM solubility [mg ml^{-1}]
1,2-dichlorobenzene	198	200	100
1,8-octanedithiol	270	1	19
di(ethylene glycol)diethyl ether	189	100	0.3
N-methyl-2-pyrrolidone	229	10	18

and gradually the concentration of OT increases in the mixture. Due to the limited solubility of PCBM in OT (Table 2), PCBM will initially form clusters and precipitate. The fact that higher surface energy of PCBM than P3HT may lead to rich PCBM distribution at the bottom of active layer when PEDOT:PSS coated ITO is used as a substrate (Fig. 5e). With a smaller amount of PCBM contained in the solution, P3HT chains are able to self-organize in an easier fashion (Fig. 5f), supported by our former study.[12] In this way, pre-formed PCBM clusters not only provide a percolation pathway for better electron transport, but also enable better hole transport in the polymer phase. As we have shown in Figure 2, the effect of OT on the crystallization kinetics of pure P3HT is rather small compared to its effect on PCBM. In other words, the composite active layer "intelligently" phase separates into the optimum morphology in one single step rather than two stages in "thermal annealing", and takes less time than "solvent annealing".

According to the proposed model, the additive in the mixture solvent approach should fulfill the following requirements: first, the compound must have lower vapor pressure than that of the primary solvent at room temperature, corresponding to a higher boiling point. Second, the compound must have lower solubility of PCBM than the solvent. Third, the compound must be miscible with solvent. Based on these requirements, we found two new additives, di(ethylene glycol)-diethyl ether (DEGDE) and *N*-methyl-2-pyrrolidone (NMP) that are effective in the P3HT:PCBM system as well. Their chemical structures are shown in Figure 1. *I–V* curves of the films processed with different mixtures under Air Mass 1.5 100 mW cm^{-2} are shown in Figure 6. The device processed without any additive shows very limited efficiency, 0.29%, which is not surprising because no "thermal annealing" or "solvent annealing" is involved. When OT is used as an additive, Jsc increases to 8.14 mA cm^{-2}, FF is doubled from 31% to 63%, and PCE is almost 10 times higher. The addition

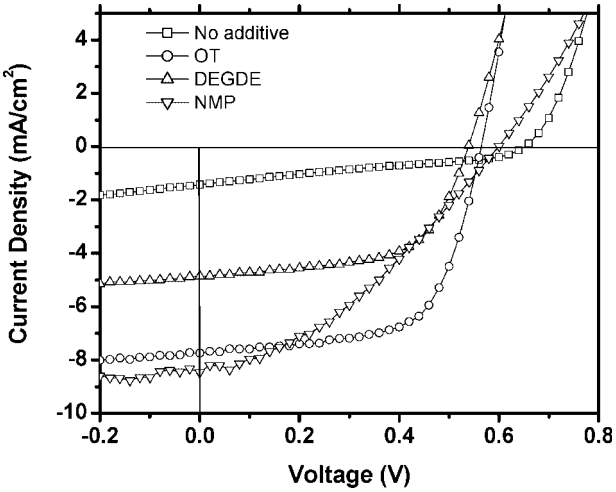

Figure 6. *I–V* curves under AM 1.5 G illumination of devices processed from a) pure DCB solvent, b) OT, c) NMP, and d) DEGDE as additive in the blend solution.

of DEGDE or NMP is also found to be effective, with PCE 5–6 times higher than those without addition. DEGDE and NMP have completely different chemical structures compared to OT, suggesting that the chemical properties of OT are irrelevant to its function. However, their physical properties (PCBM solubility and room temperature vapor pressure) are similar and consistent with our hypothesis. Notably, the boiling point of the solvent used as additive cannot be too high for obtaining better performance. This is critical since such an additive will not be removed from the film during spin-coating or later vacuum environment, and thermal treatment is required to remove the residue. As shown recently by Wang et al., oleic acid (boiling point 360 °C) was used as a ''surfactant'' to enhance performance;[35] however, surfactant alone cannot improve the performance and ''thermal annealing'' at 155 °C must be used for better performance.

3. Conclusions

In summary, the present work aims to provide a deeper understanding of how solvent mixture leads to the optimized morphology formation in polymer solar cells and identified the relevant parameters such as solubility and vapor pressure for the additive. Polymer ordering and PCBM clustering were observed in AFM and TEM images. XPS show slight phase separation in the vertical direction and polymer enrichment on the surface. A proposed model is established to explain the above observations: during the spin-coating process, the dissimilar solvent mixture can facilitate PCBM cluster formation and subsequently lead to the ''intelligent'' phase separation of the active layer into an optimum morphology. The model is further validated by discovering two new additives to show the ability to improve polymer solar cell performance as well, demonstrating the potency and versatility of the mixture solvent approach for better photovoltaic applications.

4. Experimental

OT was purchased from Sigma–Aldrich and has a boiling point of 270 °C. The typical solution used in this study for spin-coating active layer was prepared as following: P3HT (purchased from Rieke Metals, 4002E) was first dissolved in 1,2-dichlorobenezene (DCB) to make 20 mg ml^{-1} solution, followed by blending with PCBM (purchased from Nano-C) in 1:1 wt ratio. The blend solution was stirred for ~10 h at 50 °C in a glove box. A 10 μl amount of OT was added to 1 ml P3HT:PCBM solution, and then stirred for another 1 hr. Considering the density of OT (0.97 g cm^{-3}), 1 ml DCB solvent contains 20 mg P3HT, 20 mg PCBM and 9.7 mg OT. Polymer solar cell devices were fabricated on indium-tin oxide (ITO) coated glass substrates. After spin-coating a 30 nm layer of poly(3,4-ethylene dioxythiophene): poly(styrenesulfonate), the blend solution was spin-coated at 2000 rpm. The thickness of the film was ~100 nm, measured with a Dektak profilometer. The devices were completed by evaporation of metal electrodes Ca/Al with area of 10.5 mm^2 defined by masks. No further treatment was performed in this study. Testing was done in a N_2 filled glove box under AM 1.5G irradiation (100 mW cm^{-2}) using a Xenon lamp solar simulator calibrated with a silicon diode (with KG5 visible filter) calibrated with the assistance from the National Renewable Energy Laboratory (NREL). The spectral mismatch has been corrected. Absorption spectra were taken using a Varian Cary 50 ultraviolet-visible spectrometer. AFM images were obtained in tapping mode on a Veeco multimode scanning probe microscope. TEM images were obtained on a JEOL 1200EX machine with accelerating voltage of 80 kV. The XPS experiments were carried out in an Omicron Nanotechnology system with a base pressure of 2×10^{-10} Torr and Mg Kα radiation (1253.6 eV) was used as the source.

Received: December 13, 2007
Revised: January 25, 2008
Published online: June 10, 2008

[1] N. S. Sariciftci, L. B. Smilowitz, A. J. Heeger, F. Wudl, *Science* **1992**, *258*, 1474.
[2] J. Y. Kim, K. Lee, N. E. Coates, D. Moses, T. Q. Nguyen, M. Dante, A. J. Heeger, *Science* **2007**, *317*, 222.
[3] E. Bundgaard, F. C. Krebs, *Sol. Energy Mater. Sol. Cells* **2007**, *91*, 954.
[4] W.-F. Wong, X. Wang, Z. He, A. B. Djurisic, C.-T. Yip, K.-Y. Cheung, H. Wang, C. S. Mak, W.-K. Chan, *Nat. Mater.* **2007**, *6*, 521.
[5] Z. Zhu, D. Waller, R. Gaudiana, M. Morana, D. Muhlbacher, M. Scharber, C. J. Brabec, *Macromolecules* **2007**, *40*, 1981.
[6] J. Hou, Z. Tan, Y. Yan, Y. He, C. Yang, Y. Li, *J. Am. Chem. Soc.* **2006**, *128*, 4911.
[7] Y. Yao, C. Shi, G. Li, V. Shrotriya, Q. Pei, Y. Yang, *Appl. Phys. Lett.* **2006**, *89*, 153507.
[8] Y. Yao, Y. Liang, V. Shrotriya, S. Xiao, L. Yu, Y. Yang, *Adv. Mater.* **2007**, *19*, 3979.
[9] P. W. M. Blom, V. D. Mihailetchi, L. J. A. Koster, D. E. Markov, *Adv. Mater.* **2007**, *19*, 1551.
[10] S. E. Shaheen, C. J. Brabec, F. Padinger, T. Fromherz, J. C. Hummelen, N. S. Sariciftci, *Appl. Phys. Lett.* **2001**, *78*, 841.
[11] X. N. Yang, J. K. J. van Duren, M. T. Rispens, J. C. Hummelen, R. A. J. Janssen, M. A. J. Michels, J. Loos, *Adv. Mater.* **2004**, *16*, 802.
[12] G. Li, Y. Yao, H. C. Yang, V. Shrotriya, G. Yang, Y. Yang, *Adv. Funct. Mater.* **2007**, *17*, 1636.
[13] V. Shrotriya, Y. Yao, G. Li, Y. Yang, *Appl. Phys. Lett.* **2006**, *89*, 063505.
[14] F. Padinger, R. S. Rittberger, N. S. Sariciftci, *Adv. Funct. Mater.* **2003**, *13*, 85.
[15] G. Li, V. Shrotriya, J. Huang, Y. Yao, T. Moriarty, K. Emery, Y. Yang, *Nat. Mater.* **2005**, *4*, 864.
[16] J. Gilot, M. M. Wienk, R. A. J. Janssen, *Appl. Phys. Lett.* **2007**, *90*, 143512.
[17] G. Li, C.-W. Chu, V. Shrotriya, J. Huang, Y. Yang, *Appl. Phys. Lett.* **2006**, *88*, 253503.
[18] J. Y. Kim, S. H. Kim, H.-H. Lee, K. Lee, W. L. Ma, X. Gong, A. J. Heeger, *Adv. Mater.* **2006**, *18*, 572.
[19] G. Yu, J. Gao, J. C. Hummelen, F. Wudl, A. J. Heeger, *Science* **1995**, *270*, 1789.
[20] J. J. M. Halls, C. A. Walsh, N. C. Greenham, E. A. Marseglia, R. H. Friend, S. C. Moratti, A. B. Holmes, *Nature* **1995**, *376*, 498.
[21] H. Hoppe, N. S. Sariciftci, *J. Mater. Chem.* **2006**, *16*, 45.
[22] T. Erb, U. Zhokhavets, G. Gobsch, S. Raleva, B. Stuhn, P. Schilinsky, C. Waldauf, C. J. Brabec, *Adv. Funct. Mater.* **2005**, *15*, 1193.
[23] W. L. Ma, C. Y. Yang, X. Gong, K. Lee, A. J. Heeger, *Adv. Funct. Mater.* **2005**, *15*, 1617.
[24] F. Zhang, K. G. Jespersen, C. Bjorstrom, M. Svensson, M. R. Andersson, V. Sundstrom, K. Magnusson, E. Moons, A. Yartsev, O. Inganas, *Adv. Funct. Mater.* **2006**, *16*, 667.

ADVANCED FUNCTIONAL MATERIALS

[25] J. Peet, C. Soci, R. C. Coffin, T. Q. Nguyen, A. Mikhailovsky, D. Moses, G. C. Bazan, *Appl. Phys. Lett.* **2006**, *89*, 252105.
[26] J. Peet, J. Y. Kim, N. E. Coates, W. L. Ma, D. Moses, A. J. Heeger, G. C. Bazan, *Nat. Mater.* **2007**, *6*, 497.
[27] P. J. Brown, D. S. Thomas, A. Kohler, J. S. Wilson, J. S. Kim, C. M. Ramsdale, H. Sirringhaus, R. H. Friend, *Phys. Rev. B* **2003**, *67*, 064203.
[28] H. Sirringhaus, P. J. Brown, R. H. Friend, M. M. Nielsen, K. Bechgaard, B. M. W. Langeveld-Voss, A. J. H. Spiering, R. A. J. Janssen, E. W. Meijer, P. Herwig, D. M. de Leeuw, *Nature* **1999**, *401*, 685.
[29] G. Li, V. Shrotriya, Y. Yao, Y. Yang, *J. Appl. Phys.* **2005**, *98*, 043704.
[30] X. N. Yang, J. Loos, *Macromolecules* **2007**, *40*, 1353.
[31] X. N. Yang, J. Loos, S. C. Veenstra, W. J. H. Verhees, M. M. Wienk, J. M. Kroon, M. A. J. Michels, R. A. J. Janssen, *Nano Lett.* **2005**, *5*, 579.
[32] C. Bjorstrom, A. Bernasik, J. Rysz, A. Budkowski, S. Nilsson, M. Svensson, M. R. Andersson, K. O. Magnusson, E. Moons, *J. Phys. Condens. Matter* **2005**, *17*, L529.
[33] S. K. M. Jonsson, E. Carlegrim, F. Zhang, W. R. Salaneck, M. Fahlman, *Jpn. J. Appl. Phys.*, *Part 1* **2005**, *44*, 3695.
[34] H. Liao, L. Chen, Z. Xu, Y. Yang, *Appl. Phys. Lett.*, in press
[35] W. Wang, H. Wu, C. Yang, C. Luo, Y. Zhang, J. Chen, Y. Cao, *Appl. Phys. Lett.* **2007**, *90*, 183512.

